Determining the Mass and Characteristic Disk Radii of Per-Emb-14 Using Rotation and Infall

Andrew Milne,[1,2] Dominique Segura-Cox,[3,2] and Stella Offner[2]

[1] Department of Physics and Astronomy, University of Iowa, Iowa City, IA 52242, USA
[2] Department of Astronomy, The University of Texas at Austin, 2515 Speedway, Stop C1400, Austin, TX 78712-1205, USA
[3] Department of Physics and Astronomy, University of Rochester, Rochester, NY 14627, USA

ABSTRACT

Class 0/I protostars are in the earliest phases of formation and are deeply embedded in their environments. The dense natal surroundings impede kinematic measurements of parameters such as protostellar masses and disk radii. We present a study of gas dynamical mass measurements of Class 0 protostar Per-Emb-14 in the Perseus Molecular Cloud. We use FERIA — a combined Keplerian disk and infalling-rotating envelope model — to create position-position-velocity cubes using a grid search method for comparison with ALMA $C^{18}O$ observations. We find a protostellar mass of 0.41 ± 0.17 $M_{\odot}$, similar to simpler Keplerian disk fitting. We also report a maximum system outer radius $R_{\rm out}$ $= 758 \pm 177$ au. However, the spatial resolution of the observations limits accuracy. We also find a centrifugal barrier radius of 430 ± 174 au, indicating Keplerian motions dominate over infall out to a relatively large radius.

1. INTRODUCTION

Per-emb-14, also known as NGC 1333 IRAS4C, is a single Class 0 protostar (distance ∼300 pc, Ortiz-León et al. 2018). Class 0 protostars remain embedded within the molecular cloud and dense envelope (Dunham et al. 2014). The envelope obscures emission from these protostars and their rotating disks. Consequently, most young protostar masses remain unknown; only a few dozen Class 0 protostellar masses have been measured via modeling the Keplerian dynamics of their disks (e.g., Tobin et al. 2012; Murillo et al. 2013; Yen et al. 2015; Aso et al. 2023). Additionally, due to the relatively unevolved state of Class 0/I protostars, disk dynamics may not be purely governed by Keplerian rotation but instead connected to the inner gas envelope through streams of infalling material (Pineda et al. 2020).

2. DATA COLLECTION

To conduct this analysis, we use ALMA observations of Per-emb-14 (Project 2017.1.01078.S) from 22 to 24 September 2018. The data were calibrated using the ALMA pipeline with the following calibrators: J0510+1800, J0237+2848 (bandpass and flux) and J0336+3218 (phase). Self-calibration was performed on the line-free dust continuum channels and the solutions applied to the line data (see also Tychoniec et al. 2020). The line data were then imaged the using natural weighting with CASA (CASA Team et al. 2022). The $C^{18}O$ (2-1) (219.560354 GHz) emission has a spectral resolution of 0.0417 km/s, a 1σ RMS noise level of 5.16 mJy/beam, and a beam size of 0.538" x 0.383" (∼161 au x 115 au at a distance of 300 pc). The rest frequency is taken from SLAIM (F. J. Lovas, private communication; Remijan et al. 2007).

3. MODEL GENERATION

We create model cubes using FERIA (Oya et al. 2022), which is a tool developed to model gas kinematics around Class 0/I protostars using Keplerian disk and infalling-rotating envelope (IRE) models. Kirkpatrick et al. (2023) previously fit the dust continuum image with a 2D-Gaussian to recover the disk position angle of 16°, inclination angle of 70.8°, and disk center of $\alpha = $ 3:29:13.552, $\delta = +$31:13.58.081. We fix these parameters and run a grid search with the following independent parameters: protostellar mass, system inner and outer radii, and centrifugal barrier radius — where the infalling envelope and Keplerian disk interface (Sakai et al. 2014). We generate model cubes of 1000×1000 pixels with 128 velocity channels centered on the target protostar's velocity. We generate three types of models: IRE-only, Keplerian-rotation-only, and blended — with both Keplerian and IRE components.

We sample protostellar mass spanning $0.1 - 1.5$ $M_{\odot}$ with 0.1 $M_{\odot}$ spacing. This is guided by the low bolometric luminosity (1.2 $L_{\odot}$, Dunham et al. 2014) as well as Kirkpatrick et al. (2023)'s purely Keplerian curve fitting technique, which obtained 0.67 $M_{\odot}$. We sample circumstellar system inner radius spanning $1 - 300$ au with 100 au spacing. We sample circumstellar disk/envelope outer radius spanning $100 - 1000$ au with 100 au spacing. Low-mass protostellar disks typically have outer radii <100 au (Tobin et al. 2018); our data are not sensitive to scales <100 au and 1000 au is a very conservative upper limit on disk size. We sample centrifugal barrier radius spanning 0-1000 au with a

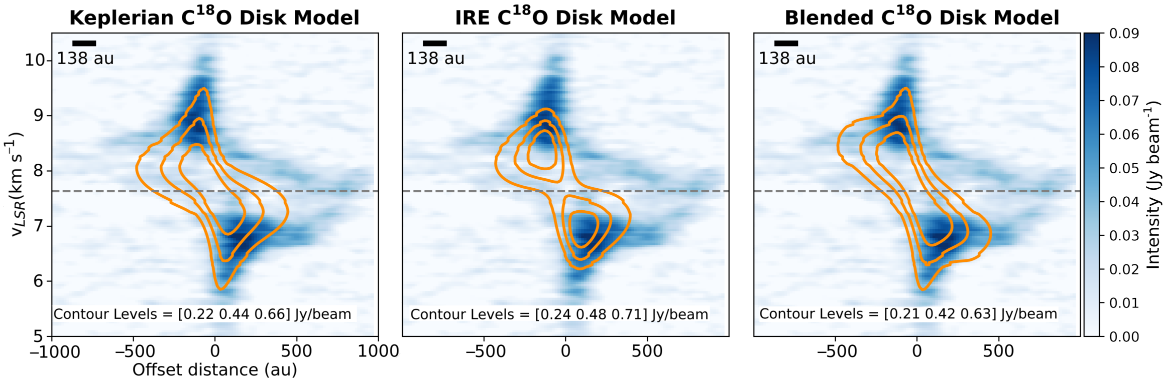

Figure 1. Overlayed position-velocity diagrams for Per-Emb-14. From left to right, the orange contours show the best-fit model for a Keplerian, infalling-rotating envelope, and blended FERIA model. ALMA observations are in blue. Contours were not corrected for radiative transfer effects.

spacing of 50 au spanning 0-500 au and 100 au from 500-1000 au. In total we generate 510 exclusively IRE models, 510 exclusively Keplerian models, and 2760 blended models.

Next we quantitatively compare the velocities to the observations voxel-by-voxel using FERIA's `CubeChi2` feature to calculate the χ^2 between two data cubes. We exclude voxels below 4σ from the comparison. Our statistical comparisons take into account only the dynamics and spatial morphology of the system; we do not directly fit for line intensities, as we do not carry out a full radiative transfer calculation since the dynamics are independent of line strength.

4. RESULTS

Figure 1 shows the lowest χ^2 model for each group overlaid to observations. Of the generated models, only a subset accurately describe Per-emb-14's dynamics. We select models below

$$\chi^2_{\rm cutoff} = 1.25 \times \min(\chi^2), \tag{1}$$

where $\min(\chi^2)$ is the lowest χ^2 we measure within our data. This excludes poor fitting models while still including a large sample population for statistical accuracy and uncertainty measurements. In total, 243 models (6.42%) fall below the threshold. These include 204 blended models and 39 Keplerian models. No IRE models fall below the threshold. 7.64% of generated Keplerian models and 7.39% of generated blended models are below the $\chi^2_{\rm cutoff}$ threshold. We estimate a protostellar mass $0.41 \pm 0.17\,M_\odot$, outer radius of 758 ± 177 au, inner radius of 1.0 ± 0.0 au (all models are smooth disks without rings), and a centrifugal barrier radius of 430 ± 174 au, where these values are the mean and standard deviation of the 243 $\chi^2_{\rm cutoff}$ models.

5. DISCUSSION

Our estimate for protostellar mass is similar to $0.67 \pm 0.01\ M_\odot$ from Kirkpatrick et al. (2023), which analytically fit Keplerian curves to Per-emb-14's $C^{18}O$ position-velocity diagram. Our lowest χ^2 values were 8.922, 9.065, and 14.357 for the Keplerian, blended, and IRE models, respectively. This suggests the envelope plays a smaller role in disk dynamics; while including an IRE component better reflects the environment, it does not significantly affect model accuracy.

While mass is well constrained, disk radii parameters have large variance. Higher spatial resolution data would better define the disk outer edge. Consequently, the disk radii should be interpreted as conservative limits on disk size.

Facilities: ALMA

Software: FERIA Oya et al. (2022)

ACKNOWLEDGMENTS

This work is supported by NSF REU grant AST-2244278 (PI: Jogee). Segura-Cox is supported by NSF AAPF award AST-2102405. Offner is supported by NSF AAG-2107942.

REFERENCES

Aso, Y., Kwon, W., Ohashi, N., et al. 2023, ApJ, 954, 101, doi: 10.3847/1538-4357/ace624

CASA Team, Bean, B., Bhatnagar, S., et al. 2022, PASP, 134, 114501, doi: 10.1088/1538-3873/ac9642

Dunham, M. M., Stutz, A. M., Allen, L. E., et al. 2014, in PPVI, ed. Beuther, Klessen, Dullemond, & Henning, 195–218, doi: 10.2458/azu_uapress_9780816531240-ch009

Kirkpatrick, C., Segura-Cox, D., & Offner, S. 2023, in AAS Meeting Abstracts, Vol. 242, 207.01

Murillo, N. M., Lai, S.-P., Bruderer, S., Harsono, D., & van Dishoeck, E. F. 2013, A&A, 560, A103, doi: 10.1051/0004-6361/201322537

Ortiz-León, G. N., Loinard, L., Dzib, S. A., et al. 2018, ApJ, 865, 73, doi: 10.3847/1538-4357/aada49

Oya, Y., Kibukawa, H., Miyake, S., & Yamamoto, S. 2022, PASP, 134, 094301, doi: 10.1088/1538-3873/ac8839

Pineda, J. E., Segura-Cox, D., Caselli, P., et al. 2020, Nature Astronomy, 4, 1158, doi: 10.1038/s41550-020-1150-z

Remijan, A. J., Markwick-Kemper, A., & ALMA Working Group on Spectral Line Frequencies. 2007, in AAS Meeting Abstracts, Vol. 211, 132.11

Sakai, N., Sakai, T., Hirota, T., et al. 2014, Nature, 507, 78, doi: 10.1038/nature13000

Tobin, J. J., Hartmann, L., Chiang, H.-F., et al. 2012, Nature, 492, 83, doi: 10.1038/nature11610

Tobin, J. J., Looney, L. W., Li, Z.-Y., et al. 2018, ApJ, 867, 43, doi: 10.3847/1538-4357/aae1f7

Tychoniec, Ł., Manara, C. F., Rosotti, G. P., et al. 2020, A&A, 640, A19, doi: 10.1051/0004-6361/202037851

Yen, H.-W., Koch, P. M., Takakuwa, S., et al. 2015, ApJ, 799, 193, doi: 10.1088/0004-637X/799/2/193